Social Distancing and Quarantine Measures in Adaptive SIR Networks

Leonhard Horstmeyer [*†], Christian Kuehn [‡§¶], and Stefan Thurner [‖]

May 2020

Abstract

In this work, we are interested in two key control measures for epidemic spreading: internal social self-distancing and externally imposed quarantine measures. We use the framework of adaptive networks, moment closure, and ordinary differential equations (ODEs) to build and study several novel models based upon susceptible-infected-recovered (SIR) dynamics. First, we compare full, computationally very expensive, adaptive network simulations with smaller-scale, computationally very fast, ODE models and find excellent agreement. Second, we discover that there is a relatively simple critical curve in parameter space for the epidemic threshold, which strongly suggests that there is compensation effect between the two mitigation measures. More precisely, as long as the social distancing and quarantine measures are sufficiently strong in tandem, then a large outbreak can be prevented. Third, we proceed to also study the total number of infected and the maximum peak during larger outbreaks using a combination of analytical estimates and numerical simulations. Also the study of large outbreaks suggests a very similar compensation effect as for the epidemic threshold. This suggests that if there is very little incentive for social distancing internal to a population, extremely drastic quarantining is required, and vice versa. Both scenarios are practically unrealistic, so our models show that only a combination of measures is likely to succeed to stop and control epidemic spreading. Fourth, for the analytical studies of the total number of infected on networks, we develop new upper bound techniques using integral estimates in combination with the application of moment closure approximation on the level of an observable. Furthermore, our general modelling shows, how many conjectures about the relevance of different network control measures can be checked and cross-validated quite elegantly and quickly, which may make it possible to adapt more rapidly to new epidemic threads such as the recent COVID-19 pandemic.

1 Introduction

2 Adaptive SIR-type Network Models

~~As outlined in Section 1, one first has to build suitable models to study the effects of practical epidemic control measures.~~ Here we ~~are particularly motivated by~~ compar~~ing~~ two quite different, yet ~~still very much~~ comparable, measures present in most epidemics: (a) social self-distancing, i.e., nodes/agents avoid infected individuals simply due to the risk of acquiring the disease themselves, and (b) external quarantine measures, which enforce the removal of infected nodes from the population. ~~In fact, it~~ is evident from data that both measures ~~have~~ played a key role during the COVID-19 pandemic. To account for the complex social structure, we start with microscopic Markov process models of susceptible-infected-recovered (SIR) dynamics on general networks with N nodes, K undirected links, and node states S, I, and R. Then we ~~are going to~~ add ~~the~~ mitigation measures to the SIR model. The well-known basic SIR rules are:

[*]equal contribution
[†]TODO: enter affiliation
[‡]equal contribution
[§]Technical University of Munich, Department of Mathematics (M8), Boltzmannstr. 3, 85748 Garching b. München, Germany
[¶]Complexity Science Hub Vienna, Josefstädter Str. 39, 1080 Vienna, Austria
[‖]TODO: enter affiliation

- (infection) I nodes infect S nodes along SI links with rate $\beta > 0$.
- (recovery/death) I nodes change to R nodes at rate $\gamma > 0$.

One ~~common~~ way to model social self-distancing, ~~which has received already major attention in the literature~~ [GDB06, SS08], is the preference of S nodes to avoid interaction with I nodes:

- (social self-distancing) SI links are re-wired to SS links at rate $w \geq 0$.

~~Hence, the~~ self-distancing/re-wiring rule makes the network fully adaptive [GS09] ~~and allows for very general network topologies. Yet,~~ the rule also takes into account that links are not lost, which mirrors the desire to keep as many social connections as possible and to ~~just optimize~~ them to mitigate risk. ~~Although~~ it is ~~relatively~~ straightforward to simulate the ~~resulting microscopic~~ Markov process on any given network, the simulations become prohibitively expensive for large N, ~~and we do not have easy analytical tools to understand the main effects of the parameters.~~ It is straightforward to use the master equation for the resulting Markov process [Nor06] and arrive at the following set of ODEs via standard techniques [KMS17]

$$\begin{array}{lllll} [\dot{S}] & = & \frac{\mathrm{d}}{\mathrm{d}t}[S] & = & -\beta[SI], \\ [\dot{I}] & = & \frac{\mathrm{d}}{\mathrm{d}t}[I] & = & \beta[SI] - \gamma[I], \\ [\dot{R}] & = & \frac{\mathrm{d}}{\mathrm{d}t}[R] & = & \gamma[I], \\ [\dot{SI}] & = & \frac{\mathrm{d}}{\mathrm{d}t}[SI] & = & -(\beta+\gamma+w)[SI] + \beta[SSI] - \beta[ISI], \\ [\dot{SS}] & = & \frac{\mathrm{d}}{\mathrm{d}t}[SS] & = & -\beta[SSI] + w\frac{[S]}{[R]+[S]}[SI], \end{array} \tag{1}$$

where ~~$[S] = [S](t)$, $[I] = [I](t)$, $[R] = [R](t)$, $[SI] = [SI](t)$, $[SS] = [SS](t)$, $[SSI] = [SSI](t)$ and $[ISI] = [ISI](t)$ are~~ expectation values of the ~~absolute~~ number of susceptible, infected and recovered nodes, of SI-~~links~~ and SS-links and of SSI-~~triplet~~ and ISI-triplet motifs ~~normalized by the total population N~~. ~~The ODEs~~ (1) ~~are~~ a variation of ~~several model elements from~~ [SS08, GDB06]. ~~In addition,~~ we do not allow recovered individuals to pass back into the susceptible compartment, which makes sense if we assume that immunity is acquir~~ing~~ upon recovery as conjectured to be true ~~on the immediate time scale of interest~~ for the COVID-19 ~~epidemic.~~ Although the ODEs (1) are actually exact in the mean-field limit [KMS17] for any graph, they are not closed as we have not written down the equations for the SSI and ISI motifs. Although these ~~equations~~ could be derived, they ~~again~~ would depend on fourth-order motifs, and so on [Kue16, HK11]. To avoid studying an infinite system of ODEs, we employ a standard moment closure pair approximation [KRM97, Kee99, KMS17, GDB06]

$$[ABC] \approx m(A,B)m(B,C)\frac{[AB][BC]}{[B]} \qquad \text{for } A,B,C \in \{S,I,R\},$$

where $m(A,B) = 2$ if $A = B$ and $m(A,B) = 1$ if $A \neq B$. With this closure, one obtains a system of ~~just~~ four ODEs for the densities $\rho_I = \frac{[I]}{N}$ and $\rho_R = \frac{[R]}{N}$ ~~of infected and recovered nodes~~ and the per-node densities of susceptible-infected and susceptible-susceptible links~~:~~

$$\begin{array}{lll} \frac{\mathrm{d}}{\mathrm{d}t}\rho_I & = & \beta\rho_{SI} - \gamma\rho_I, \\ \frac{\mathrm{d}}{\mathrm{d}t}\rho_R & = & \gamma\rho_I, \\ \frac{\mathrm{d}}{\mathrm{d}t}\rho_{SI} & = & -(\beta+\gamma+w)\rho_{SI} + \beta\rho_{SI}\frac{2\rho_{SS}-\rho_{SI}}{1-\rho_I-\rho_R}, \\ \frac{\mathrm{d}}{\mathrm{d}t}\rho_{SS} & = & -2\beta\frac{\rho_{SI}\rho_{SS}}{1-\rho_I-\rho_R} + w\left[\frac{1-\rho_I-\rho_R}{1-\rho_I}\right]\rho_{SI}. \end{array} \tag{2}$$

Here we made use of node conservation and the notation $\rho_{AB} \approx \frac{[AB]}{N}$ to emphasize that we are working with approximate per-node densities after moment closure has been applied. As such, ~~the ODEs~~ (2) only cover the aspect of social self-distancing and take into account the complex adaptive network structure via ~~a~~ second-order closure.

~~Yet, we now also want to~~ take into account quarantine effects, such as ~~the one investigated~~ in the modelling of COVID-19 in [MB20] ~~for a model without~~ network structure. Quarantine effects seem to ~~be effective to explain certain~~ features of epidemic spreading that can~~not~~ be captured by classical SIR models. ~~Keeping the conventional notation, we also~~ denote the quarantined compartment by X. The rules we use are:

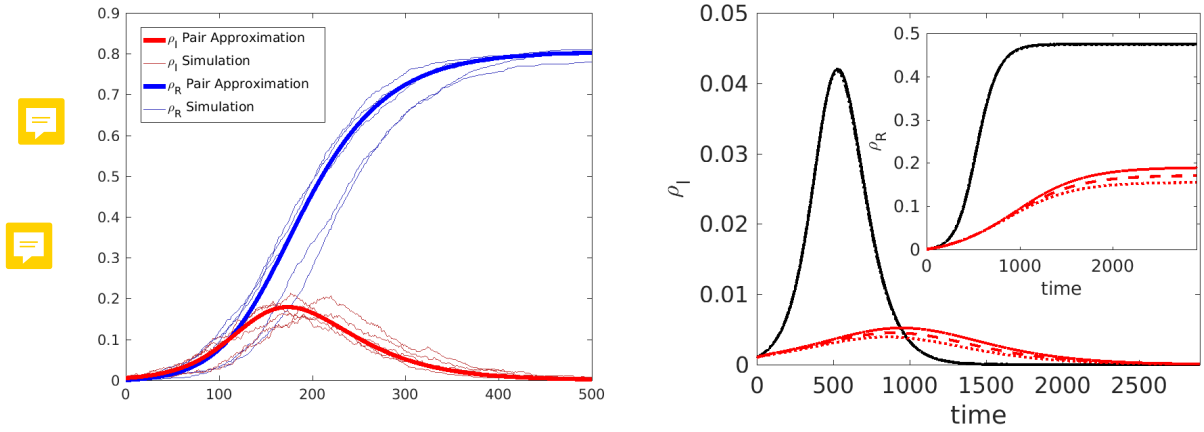

Figure 1: ~~In the left figure we can see~~ sample paths for ~~the~~ adaptive SIRX model (thin line) and the ~~P~~air approximation (thick line), ~~respectively for the density of infected~~ ρ_I and ~~the density of recovered~~ ρ_R ~~nodes, against time.~~ ~~The right plot shows the~~ pair approximations for two parameter regimes at $\beta = 0.0005$ and $w + \kappa = 0.0005$ (red) and $\beta = 0.005$ and $w + \kappa = 0.005$ (black). ~~We depict the curves~~ for a range of parameters $w/(w + \kappa) = 0.25$ (dotted), 0.5 (dashed) and 0.75 (solid). ~~The main plot shows the disease prevalence~~ ρ_I ~~and the inset shows the density of recovered nodes~~ ρ_R. ~~–~~We choose the mean degree $\mu = 15$, an initial density of $rho_I(0) = 0.001$ and a recovery rate of $\gamma = 1/40$. For the simulation we chose $N = 500$ and initial networks chosen from an Erdős-Rényi ensemble.

- (quarantine) I nodes are quarantined into a state X at rate $\kappa \geq 0$.
- (recovery of X) quarantined nodes are released into the recovered compartment R at rate $\delta > 0$.

In particular, we consider quarantining and rewiring only for the infected compartment. The expected release time from the X-compartment is $\langle T \rangle = 1/\delta$, since the rates are Poisson. However, δ does not have any effects on the amount infected individuals in this model ~~and~~ for any positive δ the amount of nodes in the recovered compartment ~~at~~ $t \to \infty$ is also independent of δ. ~~Thus for the scope of this report we take δ as a positive number. Using~~ these ~~additional~~ quarantine rules, we obtain the non-closed moment equations~~:~~

$$\begin{aligned}
\tfrac{\mathrm{d}}{\mathrm{d}t}[S] &= -\beta[SI], \\
\tfrac{\mathrm{d}}{\mathrm{d}t}[I] &= \beta[SI] - (\gamma + \kappa)[I], \\
\tfrac{\mathrm{d}}{\mathrm{d}t}[R] &= \gamma[I] + \delta[X], \\
\tfrac{\mathrm{d}}{\mathrm{d}t}[X] &= \kappa[I] - \delta[X], \\
\tfrac{\mathrm{d}}{\mathrm{d}t}[SI] &= -(\beta + \gamma + w)[SI] + \beta[SSI] - \beta[ISI] - \kappa[SI], \\
\tfrac{\mathrm{d}}{\mathrm{d}t}[SS] &= -\beta[SSI] + w\tfrac{[S]}{[R]+[S]}[SI].
\end{aligned} \tag{3}$$

More complicated variants of the rules are ~~possible and lead to slightly more involved systems as~~ discussed in Appendix A. ~~Yet, our model seems to be the first adaptive network SIR model including quarantine effects.~~ Using~~, as before, a direct~~ moment closure pair approximation, we get ~~a~~ closed system ~~of five ODEs~~

$$\begin{aligned}
\tfrac{\mathrm{d}}{\mathrm{d}t}\rho_S &= -\beta\rho_{SI}, \\
\tfrac{\mathrm{d}}{\mathrm{d}t}\rho_I &= \beta\rho_{SI} - (\kappa + \gamma)\rho_I, \\
\tfrac{\mathrm{d}}{\mathrm{d}t}\rho_R &= \gamma\rho_I + \delta(1 - \rho_S - \rho_I - \rho_R), \\
\tfrac{\mathrm{d}}{\mathrm{d}t}\rho_{SI} &= -(\beta + \gamma + w + \kappa)\rho_{SI} + \beta\rho_{SI}\tfrac{2\rho_{SS} - \rho_{SI}}{\rho_S}, \\
\tfrac{\mathrm{d}}{\mathrm{d}t}\rho_{SS} &= -2\beta\tfrac{\rho_{SI}\rho_{SS}}{\rho_S} + w\tfrac{\rho_S}{\rho_S + \rho_R}\rho_{SI}.
\end{aligned} \tag{4}$$

~~The system (3) as well as the resulting closed system (4) are our main focus and~~ allows us to compare the effects of social self-distancing and quarantine. We compare ~~our~~ model with ~~direct~~ network simulations in Figure 1. The results show excellent agreement for the vast majority of sample runs for a large part of the parameter space.

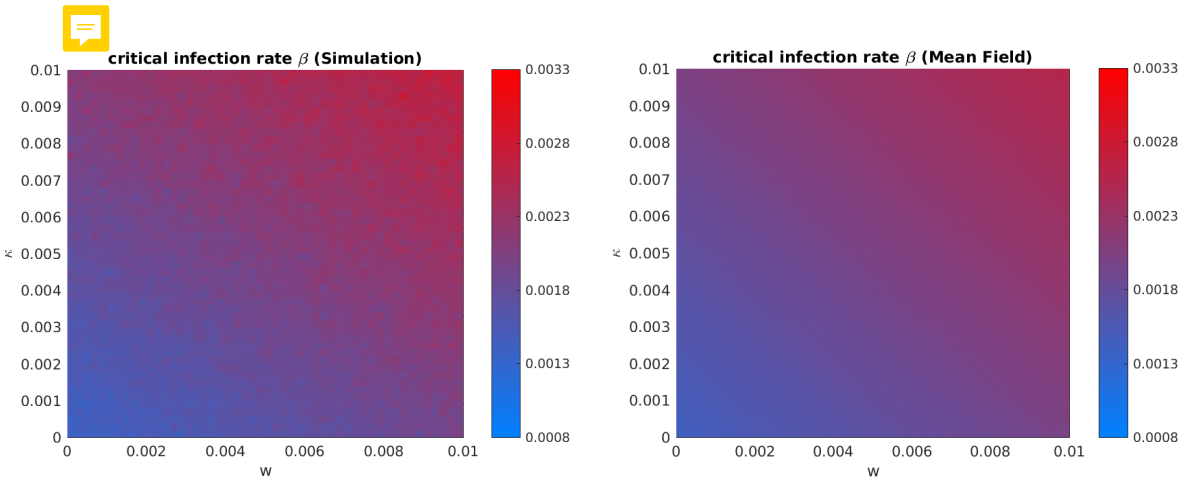

Figure 2: ~~We depict the~~ rate β at which the epidemics surpasses a threshold of $r_\infty = 0.05$. We compare ~~the~~ simulations (~~left)~~ with the mean field analysis (~~right),~~ $N = 500, \mu = 15, \gamma = 1/40, \delta = 1/100$ and $I(0) = 5$.

3 Results

~~Of course, in~~ any SIR model, in contrast to SIS or SIRS, ~~we know that~~ the epidemic eventually dies out. Hence, ~~there are~~ three questions:

a) Given an initial density of infected $I(0)$ sufficiently close to the disease-free state, does the epidemic spread, or does it ~~decay immediately to zero~~?

b) How big is the cumulative size of the epidemic outbreak? ~~This quantity is denoted by R_∞ (resp. r_∞) and~~ measures the total number of nodes at $t \to \infty$ in the recovered compartment R ~~(resp. its density)~~.

c) What is the maximum size of the epidemic $\widehat{[I]} := \max_t I(t)$, i.e., the height of the ~~biggest~~ peak?

To answer (a), the local calculation near the disease-free state is relatively simple if we have a closed ODE model. For example, ~~we~~ consider the adaptive SIR model without quarantining (2) and use the disease-free state ρ_* with

$$\rho_I = \rho_R = \rho_{SI} = 0 \quad \text{and} \quad \rho_{SS} = \mu/2,$$

i.e., also all ~~the~~ links are of type SS. Here μ is the average degree of the network, which equals $\frac{2K}{N}$ for a network with K edges. Linearizing the vector field at ρ_*, we ~~easily~~ find that for

$$\beta < \beta_c^{\text{adp}} = \frac{\gamma + w}{\mu - 1} \tag{5}$$

an epidemic dies out exponentially. A very similar calculation for the full model (4) reveals:

$$\beta < \beta_c^{\text{qurt+adp}} = \frac{\gamma + w + \kappa}{\mu - 1} \tag{6}$$

as the critical threshold for the infection rate. We see that on a local level near ρ_*, the effects of self-distancing and quarantine ~~have a very~~ comparable ~~effect as~~ the rates of both processes lower the critical threshold ~~linearly~~.

These results are ~~also~~ completely consistent with numerics. Figure 2 shows the rate β at which we record an epidemic outbreak/growth for direct network simulation as well as for numerical integration of the mean-field ODEs. The linear layered structured in the (w, κ)-diagram expected from (6) is clearly visible ~~on~~ the ~~network~~ simulation and the ODE integration levels. This ~~effectively~~ answers questions (a) ~~above,~~ and ~~tells us~~ that ~~we expect~~ a combination of measures ~~to~~ be effective to contain a disease early on. Since it is often ~~not~~ realistic ~~for a novel disease~~ that social self-distancing ~~can be expected to be fully effective~~ early on, our

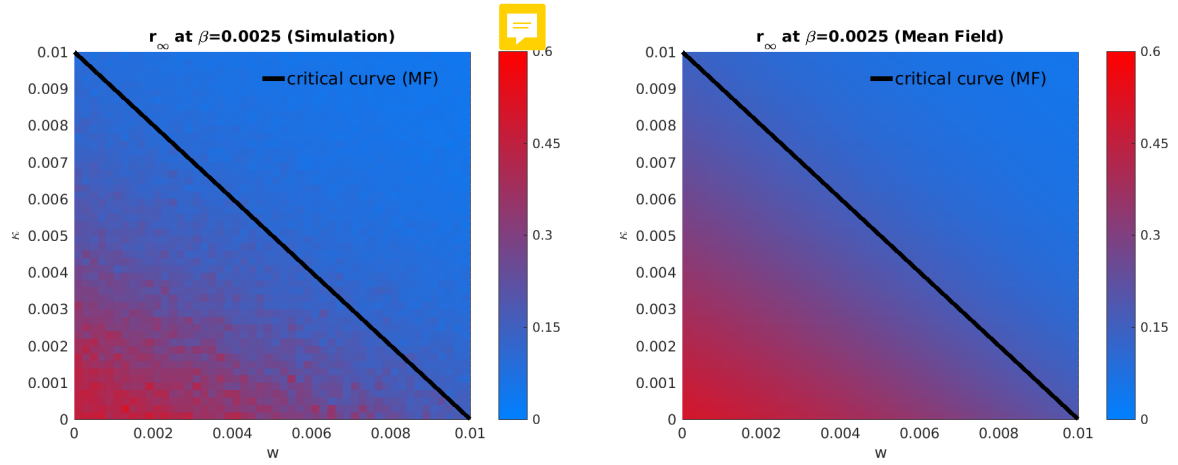

Figure 3: ~~We depict the~~ final fraction of recovered individuals r_∞ at an infection rate of $\beta = 0.0025$. We compare the simulations (~~left~~) with the mean field analysis (~~right~~) and indicate the critical curve, as calculated from (6). Again $N = 500, \mu = 15, \gamma = 1/40, \delta = 1/100$ and $I(0) = 5$.

SIR model suggests that one has to compensate and be more ~~drastic in~~ quarantine measures of infected individuals in the early phase.

~~Yet,~~ the local structure near the disease-free state only yields a partial picture ~~for~~ SIR models. In fact, one does observe epidemic outbreaks for SIR-type dynamics ~~in which case~~ we ~~need to~~ study r_∞ to answer our second question. Figure 3 shows r_∞ for a range of values near the epidemic transition in the (w, κ)-plane. We compare numerical simulations that estimate $\langle \lim_{t\to\infty} R(t)/N \rangle$ with the pair approximation $\rho_{R,\infty} := \lim_{t\to\infty} \rho_R(t)$ of ~~equation~~ (4).

~~Our~~ numerical results ~~show that there seems to exist~~ another linear relation between ~~the control~~ parameters w and κ. In general, it is impossible to get an exact formula for the maximal epidemic outbreak for an arbitrary model for SIR-type dynamics on complex networks. Yet, we can arrive at an implicit formula starting with ~~our~~ adaptive SIRX model (3). We denote the expected final number of recovered individuals by $R_\infty := \lim_{t\to\infty} [R](t)$ and write it as

$$R_\infty = R_\infty - [R](0) = \int_0^\infty [\dot{R}] \, \mathrm{d}t,$$

where we used ~~that~~ $[R](0) = 0$. ~~We also omit the argument t of the last integrand for brevity. Then we~~ use the differential equation for $[R]$ and ~~simply~~ insert it to get

$$R_\infty = \gamma \int_0^\infty [I] \, \mathrm{d}t + \delta \int_0^\infty [X] \, \mathrm{d}t.$$

Now we have two unknown integrals~~, which would suffice~~ to calculate r_∞. Using the same idea as for $[R]$, we ~~easily~~ find for $[I]$ and $[X]$:

$$\begin{aligned} 0 - [I](0) &= \int_0^\infty [\dot{I}] \, \mathrm{d}t = \beta \int_0^\infty [SI] \, \mathrm{d}t - (\kappa + \gamma) \int_0^\infty [I] \, \mathrm{d}t \\ 0 &= \int_0^\infty [\dot{X}] \, \mathrm{d}t = \kappa \int_0^\infty [I] \, \mathrm{d}t - \delta \int_0^\infty [X] \, \mathrm{d}t, \end{aligned}$$

as there can~~not~~ be any quarantined infected nodes in the beginning or at the end of the epidemic. Using the ODE for $[I]$, we get

$$R_\infty = \gamma \int_0^\infty [I] \, \mathrm{d}t + \kappa \int_0^\infty [I] \, \mathrm{d}t = \beta \int_0^\infty [SI] \, \mathrm{d}t + [I](0).$$

Now several observations are ~~already~~ evident. The procedure generically does not terminate on the infinite network level as in generic cases, we expect that all motifs could eventually occur. This means ~~we can~~ without

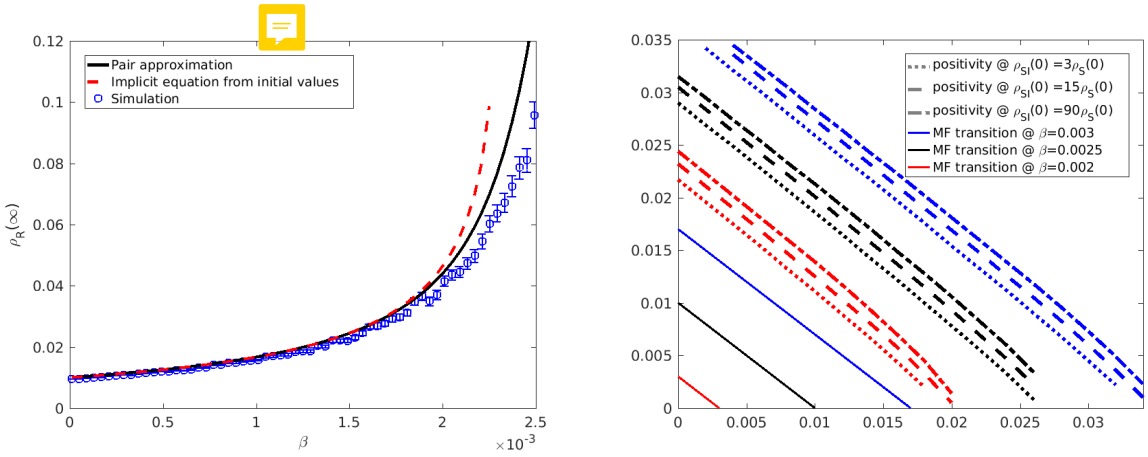

Figure 4: ~~In the left figure we depict the~~ approximation of r_∞ for the adaptive SIRX model via the ~~Pair Approximation~~ (4), the implicit ~~equation~~ (9) and ~~via repeated~~ simulation ~~of the stochastic dynamics~~. ~~In the right figure we can see the~~ boundaries of the positivity region (where $\dot{\rho}_{SI} - 2\dot{\rho}_{SS} \geq 0$ holds) in the (w, κ)-parameter space. ~~The boundaries are shown~~ for different infection rates and ~~different~~ initial conditions of the SI-link density. The mean field scenario with $\rho_{SI}(0) = \mu\rho_S(0)$ is shown as a dashed line. A scenario with dis-proportionally many initial SI-links compared to the mean field with $\rho_{SI}(0) = 6\mu\rho_S(0)$ is shown ~~as a~~ dotted line and a scenario with ~~very~~ few SI-links $\rho_{SI}(0) = (\mu/5)\rho_S(0)$ is ~~shown as~~ a dash-dotted line. The infection rates are $\beta = 0.003$ (blue), $\beta = 0.0025$ (black) and $\beta = 0.002$ (red) from top to bottom. The positivity regi~~on~~ reaches from low values of w and κ up to the respective borders. One ~~may see~~ that the ~~Mean field (MF)~~ transition curves are all within the positivity region. As before $\mu = 15$ (need to dig out the parameters again. And maybe in the positivity plot I should show the regions as well as the borders, not only the borders)

further assumptions only expect an infinite series expression for R_∞ or obtain upper or lower bounds. ~~Yet,~~ the infinite series and particularly ~~also~~ upper bounds ~~could still be very~~ informative as they ~~can~~ display the influence of the ~~different~~ parameters ~~quite clearly~~ and ~~also~~ link them to higher-order network motifs. Indeed, at the next step, the expected number of links comes into play. We get

$$0 - [SI](0) = \int_0^\infty [\dot{SI}]\ \mathrm{d}t = -(\beta + \gamma + w + \kappa) \int_0^\infty [SI]\ \mathrm{d}t + \beta \int_0^\infty [SSI]\ \mathrm{d}t - \beta \int_0^\infty [ISI]\ \mathrm{d}t,$$

~~where we have omitted the t-argument in the integrals on the right-hand side for notational simplicity.~~ ~~So~~ ~~we~~ obtain

$$R_\infty = [I](0) + \frac{\beta}{\beta + \gamma + w + \kappa}[SI](0) + \frac{\beta^2}{\beta + \gamma + w + \kappa} \int_0^\infty \Big([SSI] - [ISI] \Big)\ \mathrm{d}t. \tag{7}$$

~~In particular, we now observe that the~~ infinite sum ~~we are going to obtain always is going to~~ yield new motif terms involving infected nodes at every step ~~at the time~~ $t = 0$. This ~~is natural but shows~~ the key importance of the network structure. ~~Even at this step, one sees that a very~~ highly connected first cluster of infected nodes yields a large number of SI-links and thereby a large final outbreak size. ~~Now we~~ could carry ~~out~~ this procedure to obtain an infinite series formally but this does not give any concrete quantitative approximations. ~~So~~ we aim for an upper bound of the total number of infected/recovered.

Let us ~~now~~ impose the moment closure pair approximation *directly on* ~~equation~~ (7), using the approximate~~d~~ densities $\rho_I, \rho_R, \rho_{SI}$ and ρ_{SS} of the closed ~~equations~~ (4). ~~Then we~~ get an approximation ~~of~~ r_∞ in terms of $\rho_{R,\infty} := \lim_{t\to\infty} \rho_R(t)$

$$r_\infty \approx \rho_{R,\infty} = \rho_I(0) + \frac{\beta}{\beta + \gamma + w + \kappa}\rho_{SI}(0) + \frac{\beta}{\beta + \gamma + w + \kappa} \int_0^\infty \beta \frac{\rho_{SI}}{\rho_S} \Big(2\rho_{SS} - \rho_{SI} \Big)\ \mathrm{d}t. \tag{8}$$

Using that $\beta\rho_{SI} = -\dot{\rho}_S$ and applying the logarithmic derivative gives

$$\rho_{R,\infty} \approx K_0 + \frac{\beta}{\beta+\gamma+w+\kappa}\int_0^\infty -\frac{\mathrm{d}}{\mathrm{d}t}(\ln(\rho_S))\Big(2\rho_{SS}-\rho_{SI}\Big)\,\mathrm{d}t,$$

where $K_0 := \rho_I(0) + \frac{\beta}{\beta+\gamma+w+\kappa}\rho_{SI}(0) > 0$. Using integration by parts and $\ln(x) = -|\ln(x)|$ for $x \in (0,1]$ yields

$$\rho_{R,\infty} = K_0 + \frac{\beta}{\beta+\gamma+w+\kappa}\left(-\ln(\rho_S)\Big(2\rho_{SS}-\rho_{SI}\Big)\Big|_0^\infty - \int_0^\infty |\ln(\rho_S)|\Big(2\dot{\rho}_{SS}-\dot{\rho}_{SI}\Big)\,\mathrm{d}t\right)$$

Next, we use $|\ln(\rho_S(t))| \geq |\ln(\rho_{S,\infty})| = \ln(1-\rho_{R,\infty})$ and we make the assumption that $2\dot{\rho}_{SS} - \dot{\rho}_{SI} \leq 0$ for all times (see further for justification). Then we obtain the bound

$$\begin{aligned}
\rho_{R,\infty} &\leq K_0 + \frac{\beta}{\beta+\gamma+w+\kappa}\left(-\ln(\rho_S)\Big(2\rho_{SS}-\rho_{SI}\Big)\Big|_0^\infty + \ln\Big(1-\rho_{R,\infty}\Big)\int_0^\infty \Big(2\dot{\rho}_{SS}-\dot{\rho}_{SI}\Big)\,\mathrm{d}t\right)\\
&= K_0 + \frac{\beta}{\beta+\gamma+w+\kappa}\Bigg(-\ln\Big(1-\rho_{R,\infty}\Big)2\rho_{SS}(\infty) + \ln\Big(1-\rho_I(0)\Big)\Big(2\rho_{SS}(0)-\rho_{SI}(0)\Big)\\
&\qquad + \ln\Big(1-\rho_{R,\infty}\Big)\Big(2\rho_{SS}(\infty)-2\rho_{SS}(0)+\rho_{SI}(0)\Big)\Bigg)\\
&= K_0 + \frac{\beta}{\beta+\gamma+w+\kappa}\ln\left[\frac{1-\rho_I(0)}{1-\rho_{R,\infty}}\right](2\rho_{SS}(0)-\rho_{SI}(0))
\end{aligned}$$

Unraveling and simplifying a bit finally yields the desired upper bound

$$\rho_{R,\infty} \leq \rho_I(0) + \frac{\beta}{\beta+\gamma+w+\kappa}\left[\rho_{SI}(0) + (2\rho_{SS}(0)-\rho_{SI}(0))\ln\left[\frac{1-\rho_I(0)}{1-\rho_{R,\infty}}\right]\right]. \tag{9}$$

The bound (9) is a transcendental inequality in $\rho_{R,\infty}$. Regarding our assumption

$$\dot{\rho}_{SI} \geq 2\dot{\rho}_{SS}, \tag{10}$$

we find that it holds numerically for a broad ranges of parameters. In Figure 4(b) we show the domains of validity for the positivity assumption in the (w,κ)-plane for a range of infection rates and initial conditions. In particular the assumption holds in a neighbourhood around the critical transition.

We note that our analysis is in sharp contrast to the classical three-dimensional SIR ODE model, where an exact implicit functional relation for r_∞ can be obtained quite easily. Therefore, having a formal upper bound available such as (9) already helps us to study the parameter dependencies. In particular, we indeed see the same linear combination of the two control parameters w and κ as in the local bifurcation case near the epidemic threshold, just now they appear via an inverse. In particular, the same conclusions as regarding local epidemic spreading near the outbreak threshold are valid, when it comes to the requirement that we expect to also need a mix of quarantine and social self-distancing to keep the total number of infected r_∞ under control. Figure 4(a) shows a comparison of our upper bound for with numerical simulations of the full network as well as simulations via the mean-field ODEs derived from pair approximation. The analytical approximation as well as the mean-field approximation capture the main trend very well, which occurs if the infection rate is increased. In fact, if the total infected population is around ten percent, our approximations show that employing a well-chosen combination of quarantine and social-distancing will likely be very effective in practice, while going beyond this level, a very steep increase of the total number of infected can be observed.

Finally, we can proceed to our last question regarding the maximum peak $\widehat{[I]}$ of the number of infected, i.e., $\widehat{[I]}/N$ is the maximal fraction of the population infected at any one time over the entire duration of the epidemic. Figure 5 shows the relevant results comparing direct network simulations in Figure 5(a) with mean-field approximations in Figure 5(b). The structure of the results is very familiar in the sense that again a linear dependence between the two main parameters w and κ emerges for our main parameter ranges. Therefore, one can also conclude that using a well-tuned combination of quarantine and social self-distancing is likely to be not only effective in preventing outbreaks, or reducing the total number of infected during epidemic, but also to prevent very high peaks.

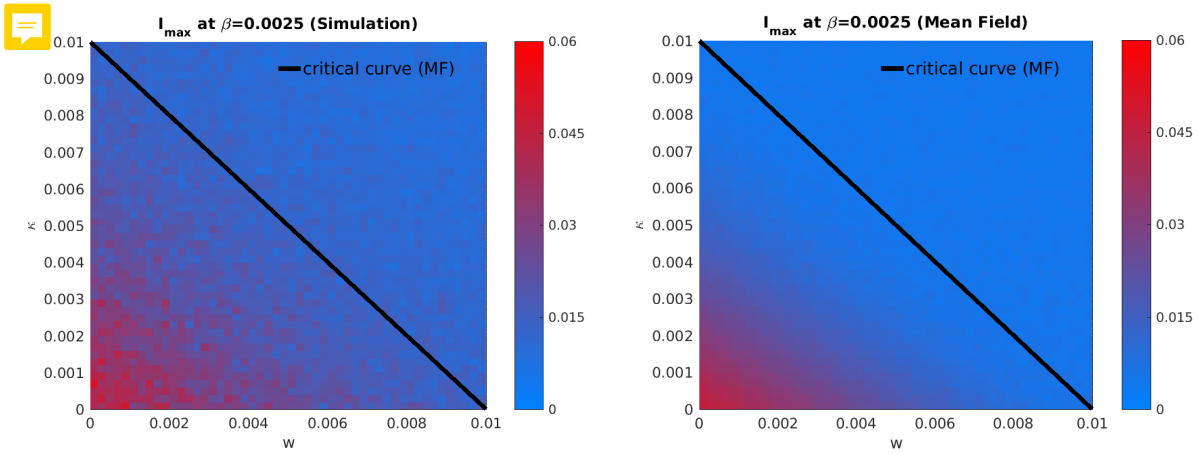

Figure 5: ~~We depict the~~ maximal fraction of infected individuals $\widehat{[I]}/N$ at an infection rate of $\beta = 0.0025$. We compare the simulations (~~left~~) with the ~~mean field~~ analysis (~~right~~) and indicate the critical curve, as calculated from (6). We see here a ~~strong~~ difference. ~~This~~ can be explained by the fact that the simulations are random processes. The average of sample path maxima over many sample paths is not the same as the maximum of the average of sample paths. The former overestimates the expectation value of ρ_I. ~~Again~~ $N = 500, \mu = 15, \gamma = 1/40, \delta = 1/100$ and $I(0) = 5$.

4 Conclusion

In this work, we have provided ~~two~~ three contributions. First, we ~~have~~ developed new adaptive network models~~, which~~ include two of the most important epidemic control measures: quarantine and social self-distancing. We ~~have also~~ derived ~~suitable~~ mean-field models via pair ~~approximation; even more detailed approximation schemes are discussed in the appendix~~. Second, we ~~have~~ analyzed ~~our~~ model via a numerical combination of direct network simulations and mean-field ODE ~~simulations,~~ which show excellent agreement. We focused on three questions regarding (a) the epidemic threshold, (b) the total number of infected individuals, and (c) the maximum peak of the epidemic. In all three cases, we ~~have~~ demonstrated for broad ~~parameter~~ ranges that the parameters controlling quarantine and social-distancing enter in a ~~very~~ comparable, ~~or even linear,~~ ~~bination~~ to control the epidemic spread. This has the practical implication that a suitable combinatio~~n~~ of these two measures is best as one cannot expect either measure to be executed perfectly in practice. Third, on a technical level we have shown a ~~completely~~ new way to provide estimates for the total infected population during an epidemic ~~via~~ using pair approximation and integral estimates directly on the level of the final infected number observable. This provides a new ~~technical~~ tool for broad class~~es~~ of epidemic models on networks.

~~In the future,~~ we ~~expect~~ that the paradigm ~~we have exhibited~~ here ~~for studying dynamic processes on networks,~~ could also be applicable to many other situations such as opinion formation models~~, where one may ask similar questions regarding the spread of an opinion~~. We ~~again~~ expect that ~~the~~ network structure is crucial as we have already demonstrated that in an epidemic setting, the change of network structure via control measures can have a drastic impact on the epidemic network dynamics.

Acknowledgements: CK acknowledges partial support by a Lichtenberg Professorship funded by the VolkswagenStiftung including the recently granted project add-on within the call “Corona Crises and Beyond”.

References

[GDB06] T. Gross, C.J. Dommar D’Lima, and B. Blasius. Epidemic dynamics on an adaptive network. *Phys. Rev. Lett.*, 96:(208701), 2006.

[GS09] T. Gross and H. Sayama, editors. *Adaptive Networks: Theory, Models and Applications*. Springer, 2009.

[HK11] T. House and M.J. Keeling. Insights from unifying modern approximations to infections on networks. *J. R. Soc. Interface*, 8:67–73, 2011.

[Kee99] M.J. Keeling. The effects of local spatial structure on epidemiological invasions. *Proc. R. Soc. London B*, 266(1421):859–867, 1999.

[KMS17] I.Z. Kiss, J. Miller, and P.L. Simon. *Mathematics of Epidemics on Networks: From Exact to Approximate Models*. Springer, 2017.

[KRM97] M.J. Keeling, D.A. Rand, and A.J. Morris. Correlation models for childhood epidemics. *Proc. R. Soc. B*, 264(1385):1149–1156, 1997.

[Kue16] C. Kuehn. Moment closure - a brief review. In E. Schöll, S. Klapp, and P. Hövel, editors, *Control of Self-Organizing Nonlinear Systems*, pages 253–271. Springer, 2016.

[MB20] B.F. Maier and D. Brockmann. Effective containment explains subexponential growth in recent confirmed COVID-19 cases in China. *Science*, 368(6492):742–746, 2020.

[Nor06] J.R. Norris. *Markov Chains*. Cambridge University Press, 2006.

[SS08] L.B. Shaw and I.B. Schwartz. Fluctuating epidemics on adaptive networks. *Phys. Rev. E*, 77:(066101), 2008.

A Moment Equations for the Adaptive and Quarantine Epidemics

I can write the appendix for these models.

A.1 Full closed equations up to second order motifs

$$\frac{\mathrm{d}}{\mathrm{d}t}[S] = -\beta[SI], \tag{11}$$
$$\frac{\mathrm{d}}{\mathrm{d}t}[I] = \beta[SI] - (\gamma+\kappa)[I], \tag{12}$$
$$\frac{\mathrm{d}}{\mathrm{d}t}[R] = \gamma[I] + \delta[X], \tag{13}$$
$$\frac{\mathrm{d}}{\mathrm{d}t}[X] = \kappa[I] - \delta[X], \tag{14}$$
$$\frac{\mathrm{d}}{\mathrm{d}t}[SI] = -(\beta+\gamma+w+\kappa)[SI] + \beta[SSI] - \beta[ISI] \tag{15}$$
$$\frac{\mathrm{d}}{\mathrm{d}t}[SS] = -\beta[SSI] + w\frac{[S]}{[R]+[S]}[SI] \tag{16}$$
$$\frac{\mathrm{d}}{\mathrm{d}t}[SR] = +\gamma[SI] + \delta[SX] - \beta[ISR] + w\frac{[R]}{[R]+[S]}[SI] \tag{17}$$
$$\frac{\mathrm{d}}{\mathrm{d}t}[SX] = -\delta[SX] - \beta[ISX] + \kappa[SI] \tag{18}$$
$$\frac{\mathrm{d}}{\mathrm{d}t}[II] = -2\gamma[II] + \beta[SI] + \beta[ISI] - 2\kappa[II] \tag{19}$$
$$\frac{\mathrm{d}}{\mathrm{d}t}[IR] = +2\gamma[II] - \gamma[IR] + \delta[IX] + \beta[ISR] - \kappa[IR] \tag{20}$$
$$\frac{\mathrm{d}}{\mathrm{d}t}[IX] = -\gamma[IX] - \delta[IX] + \beta[ISX] + 2\kappa[II] - \kappa[IX] \tag{21}$$
$$\frac{\mathrm{d}}{\mathrm{d}t}[RR] = +\gamma[IR] + \delta[RX] + \kappa[RX] \tag{22}$$
$$\frac{\mathrm{d}}{\mathrm{d}t}[RX] = +\gamma[IX] - \delta[RX] + 2\delta[XX] + \kappa[RI] \tag{23}$$
$$\frac{\mathrm{d}}{\mathrm{d}t}[XX] = -2\delta[XX] + \kappa[XI] \tag{24}$$

We see that equations for the nodes (11) till (14) depend only through $[SI]$ on the equations of the links. Equation (15) depends on itself, on $[SSI]$ and on $[ISI]$. After pair approximation there is another dependence on $[SS]$ entering, so we need (16). They are self-contained. If we now add further equations for the other link densities we obtain equations (17) till (24). We also see from equations (11) till (24), that there is node and link conservation. NOTE that there is no dependence on the average degree. And there shouldn't be. We could force it in, by redefining the variables, but why should we. So for instance if we have $\rho_S := [S]/N \in [0,1]$ for the per density of susceptibles in the population and $\rho_{SI} := [SI]/N \in [0,\mu/2]$ for the average number of $[SI]$-links per node, then we could redefine $\widehat{\rho_{SI}} := [SI]/L \in [0,1]$ as an actual density (with $\widehat{\rho_{SI}} = (2/\mu)\rho_{SI}$) and equation (11) would for then read $\frac{\mathrm{d}}{\mathrm{d}t}\rho_S = -\beta(\mu/2)\widehat{\rho_{SI}}$.

The next order can also be written down:

$$\frac{\mathrm{d}}{\mathrm{d}t}[SSI] = -r[SSI] - \kappa[SSI] - w[SSI] + w\frac{[S]}{[S]+[R]}[SI]\frac{[SI]}{[S]} - \beta[SSI] - \beta\big[S\overset{I}{S}I\big] - \beta[ISSI] \tag{25}$$
$$\frac{\mathrm{d}}{\mathrm{d}t}[ISI] = -2r[ISI] - 2\kappa[ISI] - 2w[ISI] - 2\beta[ISI] - \beta\big[I\overset{I}{S}I\big] \tag{26}$$

In terms of pair approximation densities:

$$\frac{\mathrm{d}}{\mathrm{d}t}\rho_{SSI} = -r\rho_{SSI} - \kappa\rho_{SSI} - w\rho_{SSI} + w\frac{\rho_S}{\rho_S+\rho_R}\rho_{SI}\frac{\rho_{SI}}{\rho_S} - \beta\rho_{SSI} - \beta\rho_{SI}\frac{\rho_{ISI}}{\rho_S} - \beta\rho_{SI}\frac{\rho_{SSI}}{\rho_S} \tag{27}$$

$$\frac{\mathrm{d}}{\mathrm{d}t}\rho_{ISI} = -2r\rho_{ISI} - 2\kappa\rho_{ISI} - 2w\rho_{ISI} - 2\beta\rho_{ISI} - \beta\rho_{SI}\frac{\rho_{ISI}}{\rho_S} \tag{28}$$

A.2 Adaptive SIR Model

$$\begin{aligned}
\frac{\mathrm{d}}{\mathrm{d}t}[S] &= -\beta[SI] \\
\frac{\mathrm{d}}{\mathrm{d}t}[I] &= \beta[SI] - \gamma[I] \\
\frac{\mathrm{d}}{\mathrm{d}t}[R] &= \gamma[I] \\
\frac{\mathrm{d}}{\mathrm{d}t}[SI] &= -(\beta+\gamma+w)[SI] + \beta[SSI] - \beta[ISI] \\
\frac{\mathrm{d}}{\mathrm{d}t}[SS] &= -\beta[SSI] + w * \frac{[S]}{[R]+[S]}[SI]
\end{aligned}$$

Eventually, after moment closure approximation this yields the following system for the densities:

$$\begin{aligned}
\frac{\mathrm{d}}{\mathrm{d}t}\rho_I &= \beta\rho_{SI} - \gamma\rho_I \\
\frac{\mathrm{d}}{\mathrm{d}t}\rho_R &= \gamma\rho_I \\
\frac{\mathrm{d}}{\mathrm{d}t}\rho_{SI} &\approx -(\beta+\gamma+w)\rho_{SI} + \beta\rho_{SI}\frac{2\rho_{SS}-\rho_{SI}}{1-\rho_I-\rho_R} \\
\frac{\mathrm{d}}{\mathrm{d}t}\rho_{SS} &\approx -2\beta\frac{\rho_{SI}\rho_{SS}}{1-\rho_I-\rho_R} + w\left[\frac{1-\rho_I-\rho_R}{1-\rho_I}\right]\rho_{SI}
\end{aligned}$$

We have omitted ρ_S due to node conservation.

A.3 adaptive SIR with infinite quarantine a la Brockmann 2020

Then imagine instead that not the links are removed, but that there is a state $[X]$ which represents the quarantined state. In that state disease cannot be transmitted along the link. So all those links attached to that node are removed from the pool of transmittable links. Effectively this behaves like link-removal.

$$\begin{aligned}
\frac{\mathrm{d}}{\mathrm{d}t}[S] &= -\beta[SI] - \kappa_0[S] \\
\frac{\mathrm{d}}{\mathrm{d}t}[I] &= \beta[SI] - \gamma[I] - (\kappa_0+\kappa)[I] \\
\frac{\mathrm{d}}{\mathrm{d}t}[R] &= \gamma[I] \\
\frac{\mathrm{d}}{\mathrm{d}t}[X] &= \kappa_0[S] + (\kappa_0+\kappa)[I] \\
\frac{\mathrm{d}}{\mathrm{d}t}[SI] &= -(\beta+\gamma+w)[SI] + \beta[SSI] - \beta[ISI] - 2\kappa_0[SI] - \kappa[SI] \\
\frac{\mathrm{d}}{\mathrm{d}t}[SS] &= -\beta[SSI] + w * \frac{[S]}{[R]+[S]}[SI] - 2\kappa_0[SS]
\end{aligned}$$

This latter model has the following representation:

$$\begin{aligned}
\frac{\mathrm{d}}{\mathrm{d}t}\rho_S &= -\beta\rho_{SI} - \kappa_0\rho_S \\
\frac{\mathrm{d}}{\mathrm{d}t}\rho_I &= \beta\rho_{SI} - \gamma\rho_I - (\kappa_0+\kappa)\rho_I \\
\frac{\mathrm{d}}{\mathrm{d}t}\rho_R &= \gamma\rho_I \\
\frac{\mathrm{d}}{\mathrm{d}t}\rho_{SI} &\approx -(\beta+\gamma+w+2\kappa_0+\kappa)\rho_{SI} + \beta\rho_{SI}\frac{2\rho_{SS}-\rho_{SI}}{\rho_S} \\
\frac{\mathrm{d}}{\mathrm{d}t}\rho_{SS} &\approx -2\beta\frac{\rho_{SI}\rho_{SS}}{\rho_S} + w\left[\frac{\rho_S}{\rho_S+\rho_R}\right]\rho_{SI} - 2\kappa_0\rho_{SS}
\end{aligned}$$

A.4 adaptive SIR with quarantine an return rate *delta*

Now let's consider, as before, that there is a quarantined compartment, but quarantine doesnt last for ever. We still allow for both, the susceptible population as well as the infected population to be quarantined at a rate κ_0 and $\kappa_0+\kappa$ respectively. If they are healthy quarantinees, then they'd go back into the healthy compartment. If they are infected, they go into the recovered compartment, respectively at a rate δ

So now the equations would read:

$$\begin{aligned}
\frac{\mathrm{d}}{\mathrm{d}t}[S] =& -\beta[SI] - \kappa_0[S] + \delta[X_S] \\
\frac{\mathrm{d}}{\mathrm{d}t}[I] =& \beta[SI] - \gamma[I] - (\kappa_0+\kappa)[I] \\
\frac{\mathrm{d}}{\mathrm{d}t}[R] =& \gamma[I] + \delta[X_I] \\
\frac{\mathrm{d}}{\mathrm{d}t}[X_S] =& \kappa_0[S] - \delta[X_S] \\
\frac{\mathrm{d}}{\mathrm{d}t}[X_I] =& (\kappa_0+\kappa)[I] - \delta[X_I] \\
\frac{\mathrm{d}}{\mathrm{d}t}[SI] =& -(\beta+\gamma+w)[SI] + \beta[SSI] - \beta[ISI] - 2\kappa_0[SI] - \kappa[SI] + \delta[X_SI] \\
\frac{\mathrm{d}}{\mathrm{d}t}[SS] =& -\beta[SSI] + w * \frac{[S]}{[R]+[S]}[SI] - 2\kappa_0[SS] + \delta[X_SS] \\
\frac{\mathrm{d}}{\mathrm{d}t}[X_SS] =& -\delta[X_SS] + 2\kappa_0[SS] - \beta[X_SSI] \\
\frac{\mathrm{d}}{\mathrm{d}t}[X_SI] =& -\delta[X_SI] - \gamma[X_SI] - (\kappa_0+\kappa)[X_SI] + \kappa_0[SI]
\end{aligned}$$

So putting these into 8 independent ODEs is a bit more involved:

$$
\begin{aligned}
\frac{\mathrm{d}}{\mathrm{d}t}\rho_S &= -\beta\rho_{SI} - \kappa_0\rho_S + \delta\rho_{X_s} \\
\frac{\mathrm{d}}{\mathrm{d}t}\rho_R &= +\gamma(1-\rho_R-\rho_S-\rho_{X_s}-\rho_{X_i}) + \delta\rho_{X_i} \\
\frac{\mathrm{d}}{\mathrm{d}t}\rho_{X_s} &= +\kappa_0\rho_S - \delta\rho_{X_s} \\
\frac{\mathrm{d}}{\mathrm{d}t}\rho_{X_i} &= +(\kappa_0+\kappa)(1-\rho_S-\rho_R-\rho_{X_s}-\rho_{X_i}) - \delta\rho_{X_i}
\end{aligned}
$$

$$
\begin{aligned}
\frac{\mathrm{d}}{\mathrm{d}t}\rho_{SI} &= -(\beta+\gamma+w+2\kappa_0+\kappa)\rho_{SI} + \beta\rho_{SI}\frac{2\rho_{SS}-\rho_{SI}}{\rho_S} + \delta\rho_{IX_s} \\
\frac{\mathrm{d}}{\mathrm{d}t}\rho_{SS} &= -2\beta\frac{\rho_{SI}\rho_{SS}}{\rho_S} + w\frac{\rho_S}{\rho_S+\rho_R}\rho_{SI} - 2\kappa_0\rho_{SS} + \delta\rho_{SX_s} \\
\frac{\mathrm{d}}{\mathrm{d}t}\rho_{SX_s} &= -\delta\rho_{SX_s} + 2\kappa_0\rho_{SS} - \beta\rho_{SX_s}\frac{\rho_{SI}}{\rho_S} \\
\frac{\mathrm{d}}{\mathrm{d}t}\rho_{IX_s} &= -\delta\rho_{IX_s} - \gamma\rho_{IX_s} - (\kappa_0+\kappa)\rho_{IX_s} + \kappa\rho_{SI}
\end{aligned}
$$